AJNR

Cerebral magnetic resonance image synthesis.

S A Bobman, S J Riederer, J N Lee, S A Suddarth, H Z Wang, B P Drayer and J R MacFall

AJNR Am J Neuroradiol 1985, 6 (2) 265-269
http://www.ajnr.org/content/6/2/265

Cerebral Magnetic Resonance Image Synthesis

Stuart A. Bobman[1]
Stephen J. Riederer[1]
James N. Lee[1]
Steven A. Suddarth[1]
Henry Z. Wang[1]
Burton P. Drayer[1]
James R. MacFall[2]

The authors previously described magnetic resonance (MR) image synthesis, a process that enables the investigator to manipulate imaging parameters retrospectively and generate or "synthesize" the image that corresponds to various arbitrary scanning factors. They demonstrate the validity and utility of synthetic spin-echo images in cerebral imaging. As a test of their method, spin-echo images are synthesized for echo times identical to those of the original acquired images as well as for alternate values. Subjectively, the quality of synthetic and acquired images is comparable. It is shown quantitatively for several tissue types that the reconstructed synthetic signal matches the acquired signal within the uncertainty of the acquired images. Observed and measured noise levels in the acquired and synthetic images are comparable. Because of a signal-averaging effect, the synthetic images can have a higher signal-to-noise ratio than the source images, thereby providing improved boundary definition. Applications of MR image synthesis are discussed with respect to potential reduction in scanning time. The advantages of image synthesis versus analysis of computed images are discussed.

A number of investigators recently have discussed how the observed contrast in magnetic resonance (MR) images depends both on intrinsic tissue characteristics and on extrinsic operator-selectable pulse-sequence attributes [1–7]. The intrinsic properties comprise spin density (N[H], longitudinal relaxation time (T1), and transverse relaxation time (T2). In addition to the strength of the primary magnetic field, the extrinsic scanning factors comprise the specific pulse sequence, the interpulse delay times (TE, TI), and the repetition time (TR). Because pathologic processes can alter the tissue properties and because the identity of the pathologic process often is unknown before imaging, the optimal scanning factors for visualizing a lesion also generally are unknown in advance.

One approach to overcoming this problem is automated MR image synthesis, which allows rapid retrospective optimization of contrast via interactive control of scanning factors. MR image synthesis is a three-step process. First, multiple "source" images are acquired in the usual manner with the MR scanner. Next, "computed" images of the tissue properties (N[H]), T1, and T2) are formed by subjecting the source images to computerized "fitting" routines. Finally, "synthesized" images are generated and displayed by substituting operator-selected scanning factors (TE, TI, and TR) and the computed images into the equations that describe MR signal behavior. This final step can be automated by using a high-speed digital video processor. Thus, with only one set of source images acquired with several combinations of pulse-sequence attributes, images can be synthesized for any desired scanning factors, enabling the viewer to optimize image contrast between selected tissues retrospectively. The concept of MR image synthesis has been studied by us [8–12] and by others [13–15].

If the mathematical models describing MR signal behavior are valid, the synthetic images should resemble images acquired directly from the scanner. Our initial feasibility studies [8, 9] were designed to demonstrate the utility of rapid image

Received September 19, 1984; accepted after revision November 17, 1984.

Presented at the annual meeting of the American Society of Neuroradiology, Boston, June 1984.

This work was supported by U.S. Public Health Service grant 1 R01 CA37993-01 from the National Cancer Institute, Department of Health and Human Services; by General Electric Medical Systems; and by the Whitaker Foundation.

[1] Department of Radiology, Duke University Medical Center, Durham, NC 27710. Address reprint requests to S. J. Riederer (Box 3332).

[2] General Electric Medical Systems, Milwaukee, WI 53201.

AJNR 6:265–269, March/April 1985
0195–6108/85/0602–0265

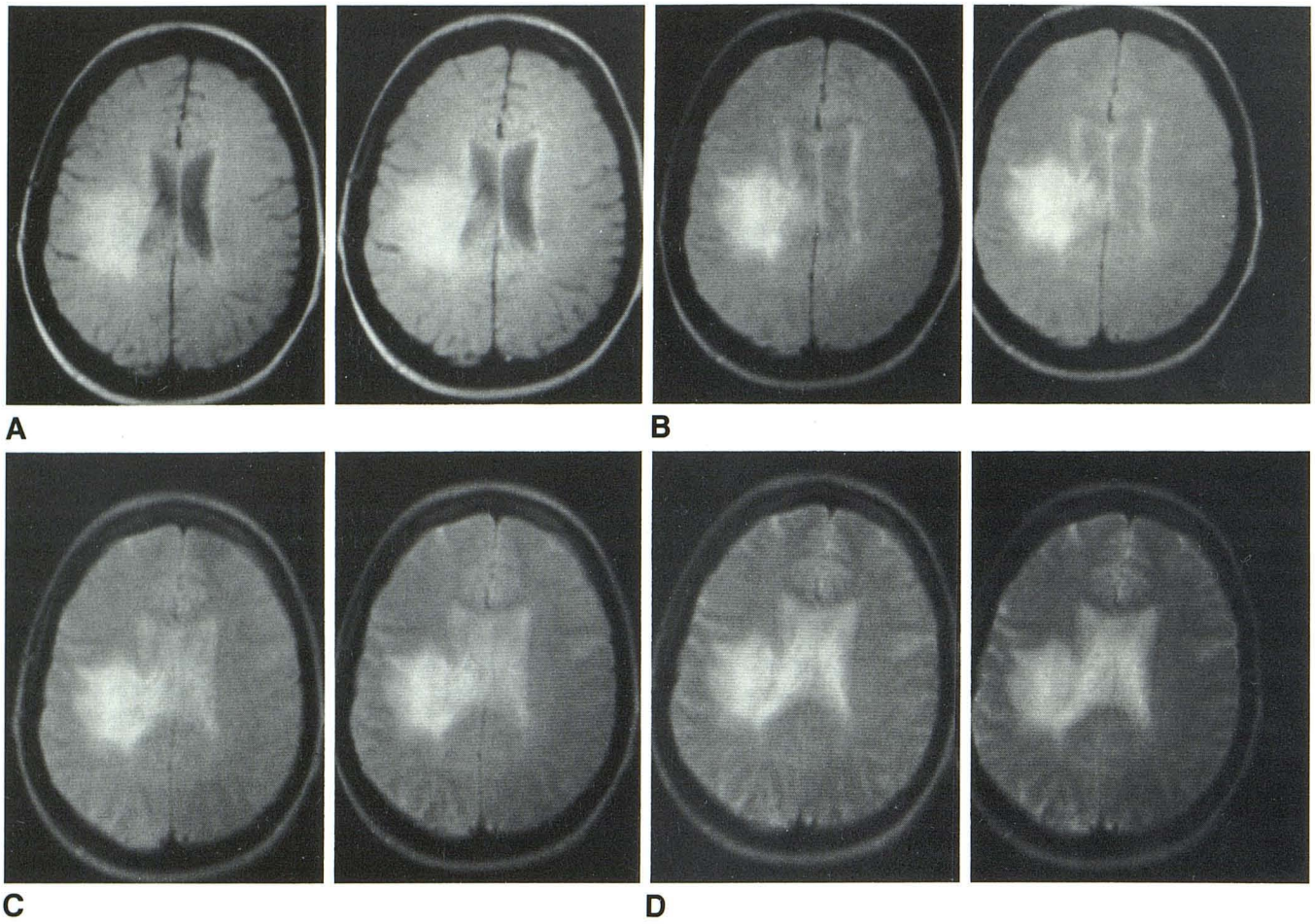

Fig. 1.—Source (*left*) and synthetic (*right*) SE images of transaxial section of head of patient with a right thalamic glioblastoma multiforme with associated vasogenic edema. TR = 1500 msec; TE = 24 (**A**), 48 (**B**), 68 (**C**), and 92 (**D**) msec.

synthesis; accordingly, precision was sacrificed for speed. The synthetic images generated were only crude representations of those acquired directly. In the current study, precise computations are performed to reproduce acquired images synthetically, to compare acquired and synthetic images both visually and numerically, and to generate images for alternate values of the echo time (TE).

Materials and Methods

Imaging was done on a General Electric superconductive MR scanner operating at 1.5 T. The source images were acquired using a multiple spin-echo (SE) pulse sequence with a repetition time (TR) of 1500 msec and TE values of 24, 48, 68, and 92 msec. Computed images were derived by first modeling the measured signal (S) as a function of TE and transverse relaxation time T2 in the standard manner [2]:

$$S \approx P \cdot e^{-TE/T2}, \quad (1)$$

in which P is defined as the pseudodensity or free induction decay, the signal that would be measured in the limit of a TE of zero (i.e., immediately after the 90° pulse). Taking the logarithm of each side of equation 1 yields the equation

$$\ln S \approx \ln P - \frac{TE}{T2}. \quad (2)$$

At each pixel a linear regression was performed to determine P and T2. That is, values for P and T2 were chosen that caused the right side of equation 2 to most closely match the left side. (Use of the logarithmic form in equation 2 versus equation 1 facilitates this process.) The resultant computed images of T2 and pseudodensity were then stored in the virtual memory of a DEC VAX-11/780 computer. On selection of a new value of TE, the T2 and pseudodensity (P) values of each pixel were entered into equation 1 using the new TE value, and the resultant image was stored in a Ramtek video processor and displayed on a monitor.

In order to assess the accuracy and precision of this method in reproducing the source images, acquired and synthetic images were compared both qualitatively and quantitatively. First, images were synthesized for TR and TE values identical to those of the acquisition. A side-by-side visual comparison was then performed between these synthetic images and the acquired source images. Next, 5- × 5-pixel regions of interest in both normal and pathologic cerebral tissue were sampled to compare source and synthetic signals at each of the four TE values. In addition, to illustrate the versatility of the process,

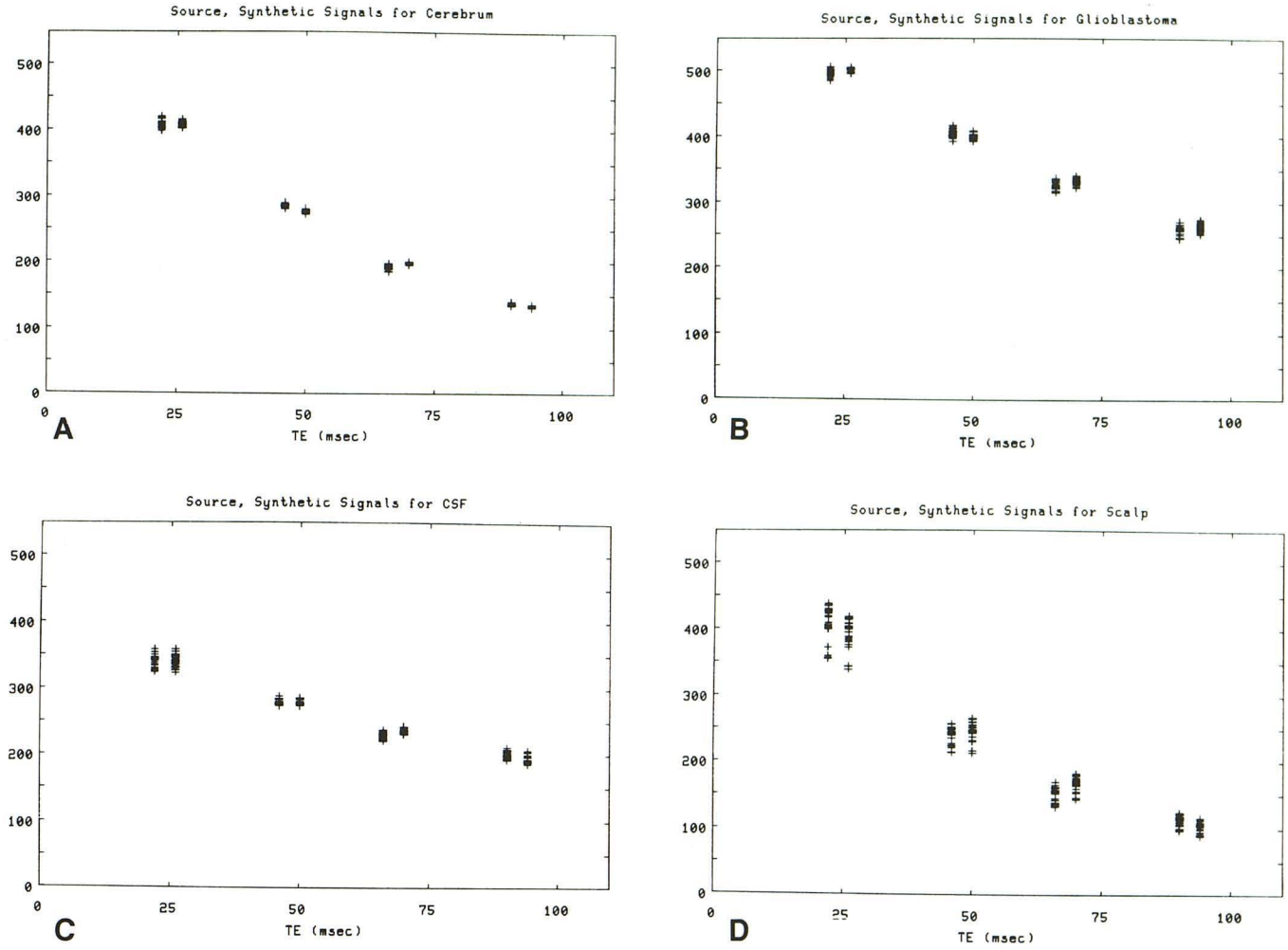

Fig. 2.—Plots of MR signals vs. each of four echo time (TE) values for 5- × 5-pixel regions of interest in cerebrum (**A**), glioblastoma (**B**), cerebrospinal fluid (**C**), and scalp (**D**). For each pair of signal sets, source values are on left and synthetic values are on right. Each horizontal bar represents signal for a single pixel.

images were then synthesized for several TE values different from those of the acquisition. Finally, the computed image of T2 was analyzed.

The patient studied was a 27-year-old woman who had presented with a 7-month history of seizures and left-sided weakness and numbness. A diagnosis of right thalamic glioblastoma multiforme was made by stereotaxic biopsy. Treatment had included radiation therapy, corticosteroids, and two courses of carmustine (BCNU). Computed tomography revealed a large enhancing right thalamic glioma with associated vasogenic edema. MR imaging defined a central area of decreased signal intensity with a partial-saturation pulse sequence having a TR of 400 msec and a TE of 27 msec. An extensive area of increased signal intensity involving almost the entire thalamic region with fingerlike extensions into the internal capsule and cerebral white matter was noted on the late SE images with long TR. A synthetic study was performed in the manner described.

Results

Figure 1 shows a set of four pairs of SE images of a transaxial section of the patient's head. In each pair of images, the acquired (source) image is on the left and the synthetic image with identical scanning factors is on the right. The synthetic images are very similar to the acquired images at TE values of 24, 48, 68, and 92 msec, respectively. Most regions of the head have been faithfully synthesized, including the glioblastoma. Moreover, the apparent signal-to-noise (S/N) ratio has not been degraded by the synthesis process at any of the four echo times. In fact, the visual noise amplitude may even be diminished in some of the synthetic images. Consequently, for early echo times, the glioblastoma appears less noisy and more sharply defined; for late echo times, the corticomedullary interface appears more distinct.

In order to quantitatively analyze the synthetic accuracy and precision in the images in figure 1, the source and synthetic MR signals were compared pixel by pixel. In figure 2, pairs of source (*left*) and synthetic (*right*) MR signals are plotted for each of the four echo times for 5- × 5-pixel regions of interest in the cerebrum, glioblastoma, cerebrospinal fluid, and scalp, respectively. For both the normal and the patho-

Fig. 3.—Source image (SE 1500/92) showing locations of regions of interest sampled for quantitative signal comparison.

logic tissues, the range and magnitude of both sets of signals are similar, indicating that the synthesis process can reproduce the acquired images within the uncertainty of the initial measurements. The regions of interest used in figure 2 are marked in figure 3. Synthetic signal behavior was similar in other regions of interest sampled.

The process and analysis presented in figures 1 and 2 show that the synthesis method can reproduce the source images with mathematical precision. An advantage of the MR image synthesis method is its ability to generate images for alternate scanning factors rapidly. Figure 4 shows synthetic SE images for the same TR value of the acquisition but with alternate TE values. Figure 4A was synthesized for a TE of zero. This image, which contains no T2 information, fails to demonstrate the tumor because the effects of altered N(H) and T1 exactly cancel each other at this repetition time. Figure 4B was synthesized for a TE of 55 msec and shows the point of isointensity between the brain and the cerebrospinal fluid in the lateral ventricles. The image in figure 4C was synthesized for a TE of 198 msec. At such a long echo time, the only regions of the image giving strong signal are those having long T2 values. Typically these regions contain fluid, such as the cerebrospinal fluid in the lateral ventricles and cortical sulci and the vasogenic edema associated with the glioblastoma. At a TE of 198 msec, the cerebrospinal fluid is more intense than the edema, unlike at a TE of 55 msec; this is consistent with a longer T2 for the cerebrospinal fluid. This is also evident in the computed image of T2 (fig. 5), which shows the lesion quite clearly.

Discussion

We have demonstrated that synthetic MR SE images compare very favorably with their acquired (source) SE images. The accuracy of the method was demonstrated directly by visual comparison of the two types of images using identical scanning factors and quantitatively by comparing acquired and synthetic MR signal values. As shown in figure 2, the average synthetic signal typically matches the source signal within the uncertainty of the acquisition. The precision of the method was demonstrated qualitatively by showing that the observed S/N ratio is not degraded in the transition process from acquired to synthetic images. Quantitatively this can be observed in figure 2, where the spread of synthetic signals (i.e., the noise level) is no wider than that of the acquired signals. In fact, the S/N ratio may even improve because of a signal-averaging effect; the four source images are in some sense "averaged" to form each new synthetic image. Display of the images in figure 1 at reduced window settings demonstrates this phenomenon clearly.

It may seem to some investigators that subjecting SE images to a curve-fitting procedure and then using the fit for recalculating or synthesizing the original images is a trivial exercise: The results *should* match the original images. But this is true only if two original SE images are used for the fit. In this case the fitted parameters—pseudodensity and T2—would be calculated deterministically from the original data, and the synthetic images would match the two acquired images exactly for all pixels. In the current study, however, four SE images were used to estimate pseudodensity and T2. In contrast to the two-point model, the resultant synthetic signal is not forced mathematically to match the acquired signal at the four echo times. Rather, the match in synthetic and acquired signals is a manifestation that the mathematical model used for the curve fit—in this case, the decaying exponential in the right side of equation 1—is an accurate description of the physical process as measured in the acquired images (the signal S in equation 1). Our results demonstrate that the model of a single exponential T2 relaxation is accurate to within the noise level useful for imaging. This study could be extended to analysis of the validity of signal dependence on T1, which would involve comparison of synthetic and acquired images using several different TR values. In this case, the pseudodensity P would be replaced by an expression specifying the signal dependence on spin density N(H), longitudinal relaxation time T1, and repetition time TR.

In discussing the utility of synthetic MR images, it is fair to question their necessity if computed images of N(H), T1, and T2 are available. Certainly, in the case of the patient presented here, the lesion is easily visualized on the computed image of T2. In fact, because this patient's tumor is isointense at a TR of 1500 msec and a TE of zero, the only reason that the lesion is visible at a TR of 1500 msec is that its T2 is prolonged. At the same level, the patient's partial-saturation scans with a TR of 400 msec and a TE of 27 msec showed a central area of decreased signal, corresponding to an area of prolonged T1. Hypothetically, if the lesion did not have an altered T2, one could in principle acquire images at several TR values and use the synthesis method to generate images for alternate values of the repetition time in an attempt to visualize the lesion. The anticipated major advantage of synthetic images over computed images is in the diagnosis of lesions that are small or that are subtle in alteration of basis quantities. In such a case, the lesion might not be visible on any of the three relatively noisy computed basis images; however, it might be possible to select scanning factors that would synthetically combine the basis images in such a manner as to increase the S/N ratio. The synthesis process allows considerable flexibility in selection of arbitrary scanning factors; the success of this strategy will depend on the degree to which statistical noise in the source images is propagated through the synthesis technique.

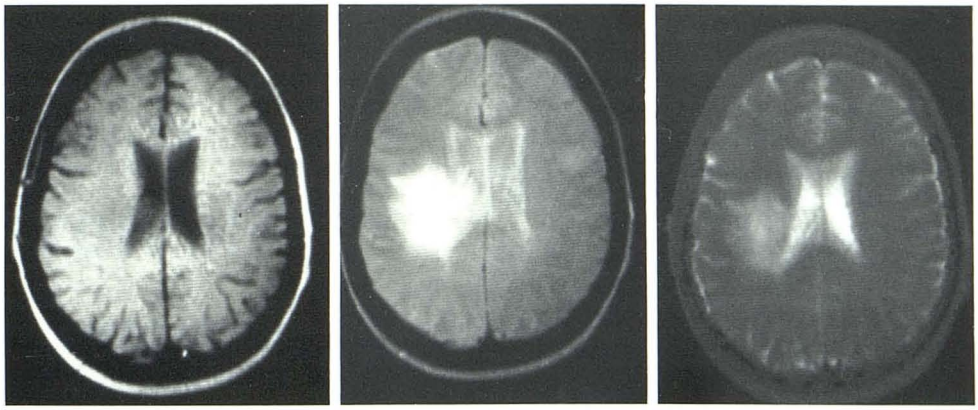

Fig. 4.—Synthetic SE images with same repetition time (TR = 1500 msec) but with various echo times: TE = zero (**A**), 55 (**B**), and 198 (**C**) msec.

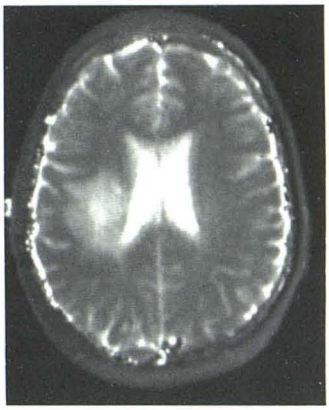

Fig. 5.—Computed T2 image.

It should be noted that if a T2 image alone were to be used as a means of diagnosis, it would still be necessary to perform comparisons (as in this study) to validate this process. That is, the results of figures 1 and 2 or their equivalent would be required to validate the use not only of synthetic MR images, but also of computed T2 images.

Another potential role of MR image synthesis is its ability to increase patient throughput. On the one hand, throughput would be expected to increase because the ability to manipulate scanning factors retrospectively could diminish the need to perform repeat scanning as provisional diagnoses changed. Even more fundamental is the possibility of reducing scanning time. MR imaging could be performed using, say, multiple SE sequences at each of two different short repetition times. These source data then could be used to synthesize images for slower (long TR) pulse sequences having higher intrinsic contrast. If carried to an extreme, such scanning-time reduction techniques would yield synthetic images having degraded accuracy and precision. However, this could be counteracted in part by the signal-averaging effect discussed above; in the example presented, eight source images were used to form one synthetic image. Moreover, if the S/N ratio were adequately high in the source images, the final image would be of diagnostic quality despite any noise increase in the synthesis process. The exact extent to which such time-reduction techniques can be carried will have to be established by additional experimentation.

REFERENCES

1. Wehrli FW, MacFall JR, Glover GH. The dependence of nuclear magnetic resonance (NMR) image contrast on intrinsic and operator-selectable parameters. *Proc SPIE* **1984**;419:256–264
2. Wehrli FW, MacFall JR, Newton TH. Parameters determining the appearance of NMR images. In: Newton TH, Potts DG, eds. *Modern neuroradiology advanced imaging techniques*, vol 2. San Anselmo: Clavadel, **1983**:81–118
3. Young IR, Bryan DTR, Payne JA, et al. Contrast in NMR imaging. Presented at the meeting of the Society for Magnetic Resonance in Medicine, San Francisco, August **1983**
4. Bryan RN, Willcott MR, Wendt RE, et al. Optimization of NMR RF pulse techniques for brain imaging. Presented at the meeting of the Radiological Society of North America, Chicago, November **1983**
5. Falke THM, Ziedses des Plantes BG, Boer JA, et al. The choice of interpulse times in NMR images. Presented at the meeting of the Radiological Society of North America, Chicago, November **1983**
6. Mitchell MR, Gibbs SJ, Partain CL, et al. Computer modeling of NMR pulse sequences. Presented at the meeting of the Radiological Society of North America, Chicago, November **1983**
7. Perman WH, Hilal SK, Simon HE, Maudsley AA. Contrast manipulation in NMR imaging. *Magnetic Resonance Imaging* **1984**;2:23–32
8. Riederer SJ, Suddarth SA, Bobman SA, Lee JN, Wang HZ, MacFall JR. Automated NMR image synthesis. Presented at the meeting of the Radiological Society of North America, Chicago, November **1983**
9. Riederer SJ, Suddarth SA, Bobman SA, Lee JN, Wang HZ, MacFall JR. Automated MR image synthesis. *Radiology* **1984**;153:203–206
10. Riederer SJ, Bobman SA, Suddarth SA, Lee JN, Wang HZ, MacFall JR. NMR image synthesis in realtime. In: Esser PD, Johnston RE, eds. *Technology of nuclear magnetic resonance*. New York: Society of Nuclear Medicine, **1984**:97–107
11. Bobman SA, Lee JN, Suddarth SA, Wang HZ, Riederer SJ, MacFall JR. Comparison of synthesized NMR images with their source images. Presented at the meeting of the Association of University Radiologists, Irvine, CA, May **1984**
12. Bobman SA, Lee JN, Wang HZ, Suddarth SA, Riederer SJ. Comparison of synthetic and experimentally acquired NMR images. Presented at the meeting of the Society for Magnetic Resonance in Medicine, New York City, August **1984**
13. Ortendahl DA, Hylton NM, Kaufman L, et al. Calculated NMR images. Presented at the meeting of the Society for Magnetic Resonance in Medicine, San Francisco, August **1983**
14. Ortendahl DA, Hylton NM, Kaufman L, et al. Calculational tools for the retrospective evaluation of NMR imaging procedures. Presented at the meeting of the Association of University Radiologists, Irvine, CA, May **1984**
15. Bielke G et al. A systematic approach to optimization of pulse sequences. In: Esser PD, Johnston RE, eds. *Technology of nuclear magnetic resonance*. New York: Society of Nuclear Medicine, **1984**:109–117